The usability evaluation and data processing methods of GNSS deformation monitoring in challenging environments

Wujiao DAI[1,*], **Yaxin WEN**[1], **Wenkun YU**[1], and **Qingshan WANG**[1]

[1] *School of Geosciences and Info-Physics, Central South University, Changsha, China, (wjdai@csu.edu.cn)*

[*] *corresponding author*

Abstract

With the continuous and increasingly in - depth application of Global Navigation Satellite System (GNSS) deformation monitoring technology, it becomes necessary to set up some monitoring points in challenging environments. These include areas close to buildings, and under trees. In such demanding settings, GNSS satellite signals are severely obstructed. This obstruction gives rise to the multipath effect, frequent diffraction, and cycle slips. These factors not only significantly degrade the quality of GNSS observation data but also present difficulties and challenges for high - precision GNSS deformation monitoring. To assess the usability of GNSS deformation monitoring in these environments, this paper first puts forward a data quality assessment method that takes into account the spatiotemporal distribution characteristics of data quality indicators. Subsequently, a comprehensive evaluation model for GNSS data quality, based on the modified VlseKriterijumska Optimizacija I Kompromisno Resenje (VIKOR), is established. This model serves as a basis for evaluating the applicability of GNSS technology. Moreover, an outlier processing method based on random sample consensus and partial ambiguity resolution is introduced to conduct a comparative analysis of the accuracy of different strategies. Finally, the results of monitoring projects for a tree-obstructed landslide demonstrate that when the environmental complexity is below 46%, an accuracy of less than 2.5 cm can be achieved. At complexity levels below 70%, the accuracy remains better than 4.0 cm. These results confirm the feasibility and effectiveness of the comprehensive evaluation model.

Keywords: Challenging Environments, GNSS, Deformation monitoring, Data quality analysis

1 Introduction

The Global Navigation Satellite System (GNSS) has become indispensable for deformation monitoring due to its high precision, continuous all-weather operation, and automation. It is widely used in landslide displacement monitoring, ground subsidence detection, structural health monitoring of large infrastructure (e.g., cross-sea bridges), and mining surface deformation monitoring(Yu et al., 2020; Hou et al., 2024; Gao et al., 2025), demonstrating significant social and economic benefits in disaster prevention and engineering safety.

Despite its advantages, GNSS performance is constrained by error sources such as multipath errors and diffraction errors, leading to traditional monitoring stations being deployed primarily in open areas. Recent studies have focused on improving GNSS applications in challenging environments (e.g., urban canyons and vegetated landslide areas). For instance, multipath mitigation methods include sidereal filtering, hemispherical models, and stochastic modeling (Zhang et al., 2022; Zhang et al., 2023a). Diffraction error suppression techniques involve 3D environmental modeling and adaptive elevation masking (Xi et al., 2023). Data quality control strategies, such as robust estimation models and multi-system ambiguity resolution(Zhang et al., 2023b; Bai et al., 2024; Wen et al., 2024), enhance monitoring accuracy in challenging conditions. These studies have strongly promoted the wide application of GNSS for deformation monitoring in challenging environments.

However, in densely vegetated landslide areas, dynamic canopy obstruction and diffraction effects cause frequent signal loss and increased noise, severely degrading GNSS data quality (Kurum et al., 2022; Ghosh et al., 2024). It is noteworthy that with the implementation of enhanced signal structures in next-generation GNSS constellations (e.g., BDS-3 and Galileo E6) and advancements in multi-frequency multi-system fusion positioning technologies, at the same time, satellite signals can partially penetrate forest canopy gaps, achieving sub-centimeter-level monitoring accuracy in partially obstructed environments has become feasible.

To evaluate the feasibility of GNSS landslide monitoring under canopy occlusion, this study conducts multi-scale obstruction experiments on a vegetated landslide. A multi-dimensional GNSS data quality evaluation system is established, integrating environmental openness and effective data distribution indicators. Data processing strategies, including carrier-to-noise ratio stochastic modeling, robust estimation, and partial ambiguity resolution, are applied to analyze monitoring performance in challenging environments.

2 Data Quality Evaluation

Observation environments directly affect GNSS data quality, which in turn GNSS data quality can reflect environmental complexity. Thus, analyzing GNSS data quality can evaluate monitoring conditions and guide processing strategies.

2.1 Data Quality Indicators

Common GNSS data quality indicators include:

- Data Integrity Rate (I): Ratio of observed datas to theoretically possible datas.
- Cycle Slip Ratio (R): Ratio of datas with cycle slips to total datas.
- Pseudorange Multipath (MP): Error caused by non-direct signals.
- Positioning Dilution of Precision (PDOP): Satellite geometry strength.

To address the limitations of these conventional metrics, this study introduces two novel indicators: Sky View Factor (SVF) and Data Distribution (D).

To more accurately reflect the spatial distribution of observations, this study introduces SVF. This indicator characterizes the openness of the monitoring environment by calculating the ratio of the actual sky sphere where satellites operate, which is not blocked by such terrain, buildings, tree canopies, when looking up from the receiver antenna to the theoretical sky sphere where satellites operate. In the landslide monitoring environment, the blocking situations are mainly divided into two categories: 1). Total blocked: For example, obstacles such as slope bodies and support structures completely block the signal, resulting in the satellite signal being unable to reach the receiver antenna at all. 2). Partial blocked: Such as the signal blocking by vegetation like forest canopies. The GNSS signal can partially penetrate the pores of the forest canopy, thus only causing a certain degree of attenuation of the signal strength. Therefore, two types of influencing factors can be considered in the calculation of the observation environment openness, and the specific calculation method of SVF is as follows:

$$\mathrm{SVF} = 1 - R(forest) * k_f - R(landslide) * k_l \quad (1)$$

where $R(forest)$ and $R(landslide)$ represent vegetation and terrain obstruction ratios, respectively. k_f is set between 0 and 1 depending on the tree type and canopy pore size and typically takes values in the range of 0.3-0.8 in landslide monitoring environments, at the same time k_l is set to 1.

From the definition of data completeness rate, it is understood that this indicator constitutes a statistical measure over the entire observation period. While it reflects the overall proportion of data loss, it fails to capture the temporal distribution characteristics of valid observational data. As illustrated in Figure 1, although all four satellites achieved 80% data completeness rates, their data distribution patterns exhibit significant disparities: Satellites 2 and 3 maintained continuous valid data segments, Satellite 1 displayed intermittent valid data throughout the period, and Satellite 4 showed fragmented data in the first half followed by continuous coverage in the latter half. So, although the data completeness rate can reflect the completeness of the data for the entire time, it is difficult to directly reflect the specific distribution of the data on the timeline.

To more accurately characterize the temporal distribution characteristics of valid data, we propose a novel evaluation indicator: Data Distribution (D). This indicator is designed to address the limitations of data integrity rate in capturing temporal distribution information. Its construction methodology is as follows:

$$D = \frac{\sqrt{n_M}}{H}\frac{STD}{Inv}, n_M > 1 \tag{2}$$

where n_M is the number of valid data epochs, H is the observed epochs, STD is the standard deviation of missing epochs, and Inv is the sampling interval.

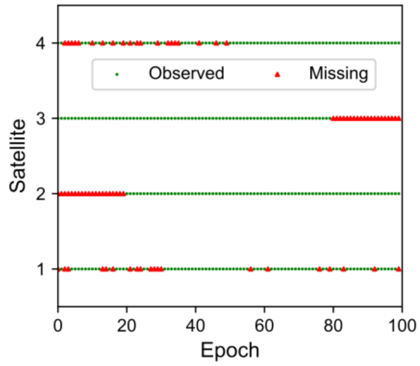

Figure 1. Schematic distribution of data from different satellites

2.2 Comprehensive Evaluation Method

Based on the integrity rate of actual observed data, a comprehensive quantitative evaluation of observation data quality is achieved by combining metrics such as cycle slip ratio and pseudomultipath. This reflects the complexity level of the monitoring environment.

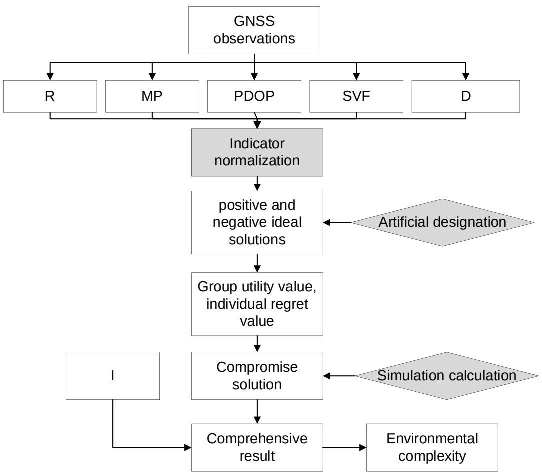

Figure 2. Comprehensive evaluation model of the complexity of the environment

In order to obtain quantitative evaluation results from multiple evaluation indicators, this study proposes a method for comprehensive quantitative assessment of monitoring station data based on the modified VIKOR (VIsekriterijum-ska optimizacija i KOm-promisno Resenje) multi-criteria compromise ranking model (Opricovic and Tzeng, 2004). VIKOR is a multi-attribute decision-making method based on ideal solutions, which evaluates alternatives by identifying the 'positive ideal solution' and 'negative ideal solution', then calculating compromise solutions for each candidate. The flowchart of the comprehensive evaluation model for observation environment complexity constructed using the VIKOR framework is shown in Figure 2. In this case, the gray-filled links are the modified parts.

The specific steps of the comprehensive data quality evaluation method are as follows:

1) **Indicator normalization.** Considering the differences in dimensions and numerical scales among evaluation indicators, standardized quantification rules are established for each indicator. Accounting for the data quality characteristics in challenging monitoring environments, threshold settings for different evaluation indicators are adjusted, and quantitative rules for each indicator are formulated：

$$\begin{gathered}
S(R) = \begin{cases} 0 & (R \geq 200) \\ \dfrac{(200 - R)}{(200 - 50)} & (50 < R < 200) \\ 1 & (R \leq 50) \end{cases} \\
S(MP) = \begin{cases} 0 & (MP \leq 50) \\ \dfrac{(MP - 50)}{(100 - 50)} & (50 < MP < 100) \\ 1 & (100 \leq MP) \end{cases} \\
S(PDOP) = \begin{cases} 0 & (PDOP \leq 1) \\ \dfrac{(PDOP - 1)}{(4 - 1)} & (1 < PDOP < 4) \\ 1 & (4 \leq PDOP < 10) \end{cases} \\
S(SVF) = \begin{cases} 0 & (SVF \geq 0.3) \\ \dfrac{(0.8 - SVF)}{(0.8 - 0.3)} & (0.3 < SVF < 0.8) \\ 1 & (0.8 \leq SVF) \end{cases} \\
S(D) = \begin{cases} 0 & (D \leq 0.2) \\ \dfrac{(D - 0.2)}{(0.8 - 0.2)} & (0.2 < D < 0.8) \\ 1 & (0.8 \leq D) \end{cases}
\end{gathered} \tag{3}$$

In the formula: $S(R)$, $S(\text{MP})$, $S(\text{PDOP})$, $S(O)$ and $S(D)$ represent the scoring quantification rules for cycle slip ratio, pseudorange multipath, PDOP, SVF, and effective data distribution, respectively. Through these quantification rules, individual indicator evaluation results for monitoring environment complexity are obtained. A smaller evaluation value indicates a more ideal monitoring environment.

2) **Determination of positive and negative ideal solutions.** The standard VIKOR method determines positive and negative ideal solutions by searching all samples to enable relative evaluation of multiple schemes. To achieve quantitative evaluation of monitoring environment complexity, this study adopts fixed positive and negative ideal solutions for quantitative assessment:

$$S_i = \sum\omega_* \times \left(\frac{S(*)^+ - S(*)_i}{S(*)^+ - S(*)^-}\right)$$
$$R_i = max\left[\omega_* \times \left(\frac{S(*)^+ - S(*)_i}{S(*)^+ - S(*)^-}\right)\right] \quad (4)$$

In the formula: $S(*)^+$ represents the positive ideal solution for the corresponding indicator, and $S(*)^-$ represents the negative ideal solution for the corresponding indicator.

To determine the weights of different indicators, this study employs simulations to quantify the impact magnitudes v_* of various indicator types.

$$\omega_* = \frac{|v_*|}{\sum|v|} \quad (5)$$

3) **Calculate the group utility value S_i and individual regret value R_i:**

$$S_i = \sum\omega_* \times \left(\frac{S(*)^+ - S(*)_i}{S(*)^+ - S(*)^-}\right)$$
$$R_i = max\left[\omega_* \times \left(\frac{S(*)^+ - S(*)_i}{S(*)^+ - S(*)^-}\right)\right] \quad (6)$$

In the formula: ω_* represents the prior weight of the corresponding evaluation indicator, and $S(*)_i$ denotes the evaluation result of the corresponding indicator for the i-th sample.

4) **Calculate the compromise solution Q_i:**

$$Q_i = v\frac{S_i - S_{\text{imin}}}{S_{\text{imax}} - S_{\text{imin}}} + (1 - v)\frac{R_i - R_{\text{imin}}}{R_{\text{imax}} - R_{\text{imin}}} \quad (7)$$

In the formula: v represents the decision mechanism coefficient, and $v \in [0,1]$. In the standard VIKOR algorithm, S_{imax}、S_{imin}、R_{imax} and R_{imin} denote the maximum and minimum group utility values, and the maximum and minimum individual regret values of the sample set, respectively. To obtain quantitative evaluation results, these values are fixed here as 1, 0, 1, and 0 accordingly.

By utilizing a compromise solution to evaluate the quality of observed data and combining it with the data integrity rate, the comprehensive result(CR) of the corresponding system is determined:

$$\text{CR}_i = 1 - (1 - Q_i) * I \quad (8)$$

The final evaluation result of environmental complexity(EC) is obtained by analyzing the data quality of different systems:

$$\text{EC} = \sum \text{CR}_i * N_{sysi} / \sum N_{sysi} \quad (9)$$

Where N_{sysi} refers to the number of satellite systems corresponding to the results.

3 Data Processing Strategies

The monitoring data was processed using the team-developed GNSS data management system (GNSSDMS). Due to impacts such as tree canopy occlusion, the GNSS data quality in such scenarios suffers from significant outliers and challenges in ambiguity resolution. To address these issues, robust estimation and Partial Ambiguity Resolution (PAR) strategies were integrated into the standard data processing workflow. Below are detailed descriptions of the stochastic model, robust estimation strategies, and PAR implementation methodologies.

3.1 Stochastic Model

Due to differences in the propagation paths of GNSS satellite signals, the interference from environments varies, leading to significant distinctions in the quality of observational data among different satellites. To effectively characterize these variations in observation accuracy, stochastic models are typically employed in GNSS data processing to weigh the observations. Commonly used stochastic models include the elevation model, carrier-to-noise ratio (C/N0C/N0)-based model, and posterior variance estimation model. Previous studies have demonstrated that the C/N_0-based stochastic model better reflects observation data quality in challenging environments (Eueler and Goad, 1991). This is because the carrier-to-noise ratio directly quantifies the relationship between received signal strength and noise levels, enabling sensitive detection of signal quality degradation caused by multipath effects, ionospheric disturbances, and signal occlusion. So, a carrier-to-noise ratio (C/N0C/N0)-based stochastic model is adopted:

$$\sigma^2 = C_i \times 10^{-\frac{C/N_0}{10}} \tag{10}$$

where $C_{L_1} = 0.002\ 24\ \mathrm{m}^2 Hz$ and $C_{L_2} = 0.000\ 77\ \mathrm{m}^2 Hz$.

3.2 Robust Estimation

In challenging environments, GNSS signals are susceptible to interference from surrounding conditions, which significantly increases the probability of multiple outliers in GNSS data. To effectively identify and mitigate these outliers, this study employs the RANSAC algorithm (Wen et al., 2024) to process outliers, thereby reducing their impact. The methodology is detailed as follows:

1) **Sampling**: Randomly select a subset of size t. To maximize the probability of obtaining a subset free of outliers, the sample size is typically set to the minimum required for estimating the parameters.
2) **Computation**: Calculate the parameters using the selected subset.
3) **Back-substitution Test**: Substitute the parameters into all samples to evaluate their consistency with the estimated values.
4) **Evaluation and Update**: Classify samples with residuals below a predefined threshold as inliers (added to the inlier set) and those exceeding the threshold as outliers (assigned to the outlier set). If the current inlier set surpasses the previous optimal, update the optimal subset.
5) **Iteration**: Repeat steps 1)– 4) until the iteration count meets the minimum requirement, then output the final results.

3.3 Partial Ambiguity Resolution

In high-precision GNSS data processing, ambiguity resolution in challenging environments has long been a critical technical challenge requiring urgent solutions. To address difficulties in ambiguity resolution under tree canopy occlusion, signal interruptions, and frequent cycle slips, this study adopts a PAR strategy to enhance the success rate and reliability of ambiguity resolution. Current mainstream PAR strategies typically select satellite subsets based on ambiguity resolution success rates, elevation angles, signal-to-noise ratios, and satellite variances (Jiang et al., 2022b). Considering the frequent signal loss and cycle slips in obstructed environments, this paper proposes a satellite subset selection strategy that accounts for tracking epochs and ambiguity variance. The core steps are as follows:

1) **Initial Ambiguity Resolution**: First, attempt to fix ambiguities for all available satellites. If successful, output the results directly.
2) **Eliminate Satellites with Few Tracking Epochs**: If the initial attempt fails, prioritize removing satellites with insufficient tracking epochs due to their higher ambiguity uncertainty.
3) **Remove Satellites with High Ambiguity Variance**: If ambiguity resolution remains unsuccessful, further eliminate satellites exhibiting large ambiguity variances to reduce noise in the ambiguity set.
4) **Termination Criteria**: Stop when ambiguities are resolved, or insufficient satellites remain.

4 Case Study

4.1 Landslide Monitoring

4.1.1 Monitoring Environment and Data Quality

To thoroughly analyze GNSS landslide monitoring performance in tree-obstructed environments, this study collected GNSS observation data from three monitoring points with varying obstruction levels on a typical landslide body in Shenzhen, China. Data acquisition at 2024-02-06. The project utilized the BYT1-8D multi-frequency multi-constellation receiver, configured with a 30-second sampling interval, to capture data from BDS, GPS, and Galileo systems.

Figure 4 illustrates the site scenarios, carrier-to-noise ratio (C/N0) spatial distributions, and obstruction maps of the three monitoring points. Based on field tree occlusion conditions, the sky visibility ratio k_f—calculated from hemispherical fisheye imagery as the pixel proportion of unobstructed sky areas—was determined to be 0.43. Table 1 summarizes the obstruction characteristics of the monitoring points. Where DB01: Primarily affected by terrain occlusion, exhibiting the highest SVF. DB02: Signals suffer from canopy-induced occlusion and diffraction, leading to intermittent data gaps and reduced C/N0. DB03: Severe tree occlusion results in the lowest SVF. Even satellites at 80° elevation angles experience significant signal interference and trajectory interruptions, causing marked C/N0 degradation.

Table 2 presents a comparative analysis of data quality across three monitoring points under different satellite system configurations, where G, C, E, GC, and GCE correspond to GPS-only, BDS-only, Galileo-only, GPS+BDS dual-system, and GPS+BDS+Galileo triple-system configurations, respectively. The table reveals that single systems (GPS or Galileo alone) observe fewer satellites, exhibit poorer satellite geometry, and yield higher PDOP. In contrast, combining GPS+BDS or GPS+BDS+Galileo significantly increases the number of observable satellites and improves PDOP.

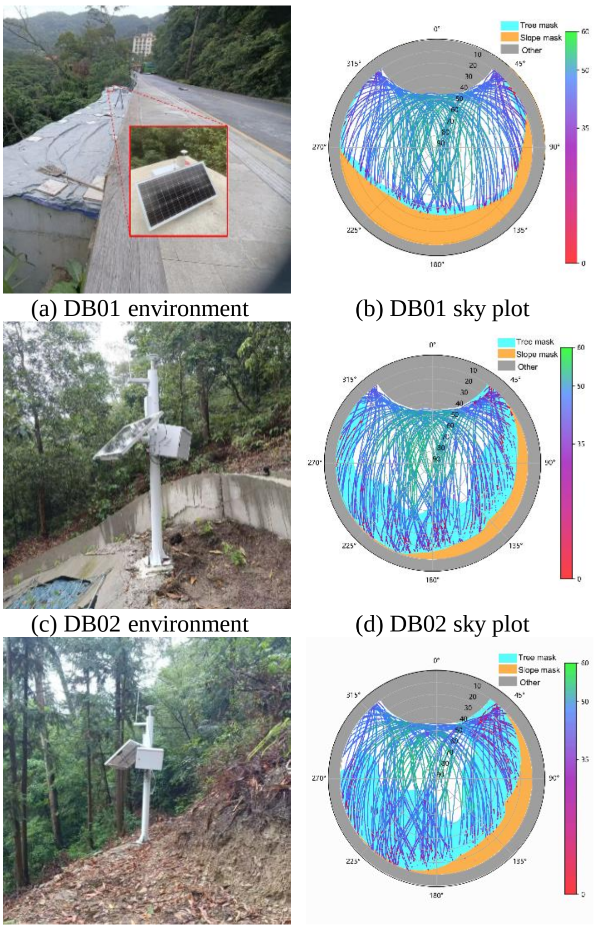

(a) DB01 environment (b) DB01 sky plot
(c) DB02 environment (d) DB02 sky plot
(e) DB03 environment (f) DB03 sky plot

Figure 3. Environmental graph of the three sites

Table 1. Obstruction Statistics

Site	Slope mask (%)	Tree mask (%)	SVF (%)
DB01	23.05	7.58	73.69
DB02	9.04	47.16	70.68
DB03	11.60	56.54	64.09

Table 2. Statistics on data quality information

Site		G	C	E	GC	GCE
	I (%)	79.5	77.9	80.3	78.4	79.0
	R	194.2	267.5	248.8	243.1	244.7
DB01	MP (cm)	62.6	48.6	65.0	54.1	55.7
	PDOP	2.8	1.8	12.0	1.3	1.3
	D	0.3	0.1	0.3	0.2	0.2
	I (%)	84.0	80.4	79.9	81.7	81.3
	R	87.4	115.0	110.4	105.5	107.8
DB02	MP (cm)	64.4	61.2	63.7	62.7	62.9
	PDOP	2.5	1.6	7.7	1.2	1.2
	D	0.5	0.3	0.6	0.4	0.4
	I (%)	83.4	84.4	79.2	84.1	83.0
	R	59.3	95.2	91.1	83.3	84.9
DB03	MP (cm)	67.1	63.6	63.7	61.4	62.0
	PDOP	2.8	1.7	13.1	1.3	1.3
	D	0.8	0.4	0.6	0.5	0.5

Notably, although the DB01 monitoring point has the lowest data integrity rate due to terrain-induced obstructions, its effective observational data quality surpasses other points owing to weaker vegetation occlusion effects. This phenomenon highlights the distinct impacts of vegetation coverage and terrain obstruction on GNSS signal quality in complex topographic environments.

Using the comprehensive evaluation model from Section 2.2, the data quality of different satellite systems and their combinations at the three sites were evaluated. The weights for each indicator were assigned based on simulation results as follows: $S(R){:}\,S(MP){:}\,S(PDOP){:}\,S(\mathrm{SVF}){:}\,S(D) = 0.26{:}\,0.10{:}\,0.42{:}\,0.10{:}\,0.12$, the decision mechanism coefficient was set to: $\upsilon = 0.5$. Detailed results are shown in Table 3. The analysis indicates that DB01 exhibits superior overall data quality, while DB03 demonstrates relatively poorer data quality. Single-system configurations (e.g., GPS) show degraded data quality due to limited satellite counts and poor PDOP values. Multi-system combinations (e.g., GPS+BDS+Galileo) significantly improve data quality. Regarding environmental complexity, DB01 has the lowest complexity, whereas DB03 operates in the most complex environment.

Table 3. Comprehensive results and environmental complexity

Site	Comprehensive results(%)					EC(%)
	G	C	E	GC	GCE	
DB01	57.4	37.4	78.7	28.2	27.7	45.9
DB02	66.0	55.4	90.1	56.8	56.0	65.0
DB03	70.8	60.9	92.6	59.6	60.0	68.8

In landslide monitoring scenarios with dual vegetation and terrain obstructions, GNSS data quality deteriorates significantly, manifesting as decreased data integrity rate, increased cycle slips, and degraded satellite geometry. With multi-system combinations (e.g., GPS+BDS+Galileo) can substantially improve satellite visibility and geometric configuration, thereby offering the possibility of high-precision landslide monitoring.

4.1.2 Monitoring Performance

For monitoring sites under three different occlusion conditions, this study utilizes observation data acquired on February 6, 2024, to perform real-time kinematic (RTK) solutions and statistically evaluates their positioning accuracy. The distances from DB01, DB02, and DB03 to the reference station are approximately 178 m, 282 m, and 321 m, respectively. Figures 5–7 display the displacement time series under different solution strategies, and Table 4 details the ambiguity fixing rates and root mean square error (RMSE) of the displacement sequences for these strategies. Here, "-R" denotes the integration of a robust strategy into the standard Kalman filter (KF), while "-RP" indicates the further incorporation of a partial ambiguity fixing strategy based on the robust Kalman filter.

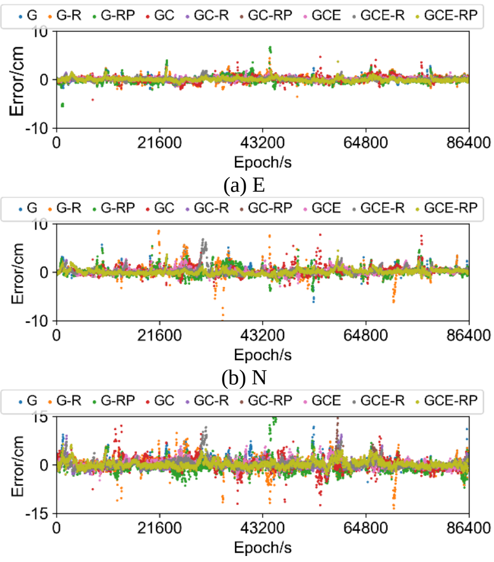

(a) E
(b) N
(c) U

Figure 4. DB01 dynamic monitoring of coordinate sequences

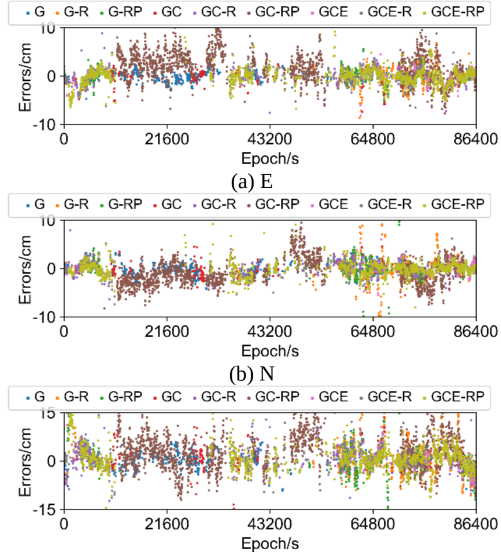

(a) E
(b) N
(c) U

Figure 5. DB02 dynamic monitoring of coordinate sequences

The dynamic results indicate that at the DB01 monitoring point with the lowest environmental complexity, the positioning accuracy of different GNSS system combinations is better than 2.5 cm. While multi-system combinations can improve accuracy, they also increase the difficulty of ambiguity resolution, potentially reducing the ambiguity fixing rate. At the more complex monitoring points DB02 and DB03, where leaf movement is frequent and the number of satellites in a single system is limited, the positioning accuracy deteriorates. Although multi-system data integration enhances available observations, it also raises the probability of gross errors and complicates ambiguity resolution. When sufficient observational data is available, employing a robust algorithm can improve accuracy to some extent. Further application of a partial ambiguity fixing algorithm can boost the ambiguity fixing rate and correspondingly enhance precision, ultimately achieving monitoring accuracy within 4 cm.

Table 4. Dynamic monitoring accuracy statistics

Site	Strategy	G		GC		GCE	
		RMSE (cm)	Fixing rate (%)	RMSE (cm)	Fixing rate (%)	RMSE (cm)	Fixing rate (%)
	KF	2.2	80.9	1.6	72.8	1.6	53.8
DB01	KF-R	2.2	92.4	1.4	95.3	1.4	96.5
	KF-RP	2.1	96.7	1.1	98.8	1.0	99.2
	KF	5.5	17.4	5.9	8.9	5.4	7.5
DB02	KF-R	6.5	30.9	4.3	33.2	4.0	40.7
	KF-RP	6.2	33.1	3.8	53.1	3.4	62.5
DB03	KF	20.2	10.9	11.9	9.8	7.3	3.0
	KF-R	30.1	19.1	6.5	43.6	4.1	45.8
	KF-RP	28.5	23.4	4.0	48.1	3.8	56.2

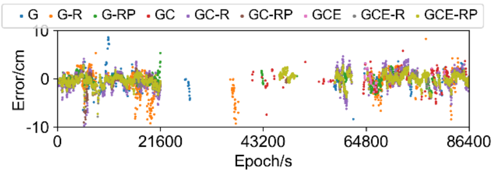

(a) E

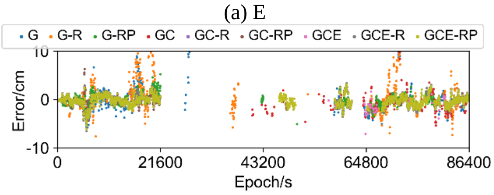

(b) N

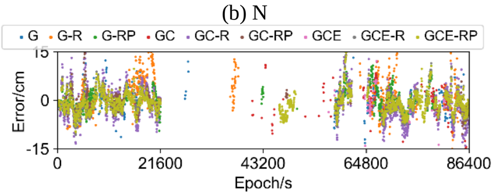

(c) U

Figure 6. DB03 dynamic monitoring of coordinate sequences

5 Conclusions

This paper conducts an in-depth analysis of landslide monitoring performance at three sites under varying tree occlusion conditions. Through comparative assessments of observation data quality and dynamic performance, the following conclusions are drawn:

1) The distribution of valid data and environmental openness can partially reflect monitoring data quality. A modified VIKOR-based multi-criteria quantitative evaluation model effectively assesses environmental complexity.

2) In challenging environments, GNSS monitoring accuracy decreases. However, strategies such as multi-system integration, robust estimation, and partial ambiguity fixing enhance precision and usability. When environmental complexity is below 46%, sub-2.5 cm is achievable. At complexity levels below 70%, accuracy remains better than 4.0 cm.

Landslide monitoring in heavily obstructed environments faces challenges like signal obstruction, increased gross errors, and ambiguity resolution difficulties. The application of artificial intelligence and machine learning technologies to GNSS data processing is expected to enable more precise identification and handling of outliers, optimize ambiguity resolution algorithms, and enhance the adaptability and accuracy of models. Additionally, the integrated development of GNSS with other technologies—such as combining GNSS with Inertial Navigation Systems (INS) can acquire richer environmental information, providing support for GNSS signal processing and precision improvement. These measures can further explore their application potential in complex environments and unlock possibilities for enhancing monitoring performance.

References

Dong Y, Zhang Z, Pang L, Dong H, Shi Y (2023) Partial ambiguity resolution considering the multipath effects in a canyon environment. Survey Review 56(396):1–16.

Eueler H-J, Goad CC (1991) On optimal filtering of GPS dual frequency observations without using orbit information. Bulletin Géodésique 65(2):130–143.

Gao R, Ye F, Odolinski R, Satirapod C, Zhang B (2025) Mitigating ionospheric scintillation effects on RTK-based long-span bridge deformation monitoring. Measurement 242:115957.

Ghosh A, Farhad MM, Boyd D, Kurum M (2024) A UGV-Based Forest Vegetation Optical Depth Mapping Using GNSS Signals. IEEE Journal of Selected Topics in Applied Earth Observations and Remote Sensing 17:5093–5105.

Hou C, Shi J, Ouyang C, Guo J, Zou J (2024) A dual-base station constraint method to improve deformation monitoring precision consistency in strip regions. Satell Navig 5(1):26.

Jiang W, Chen Y, Chen Q, Chen H, Pan Y, Liu X, Liu T (2022a) High precision deformation monitoring with integrated GNSS and ground range observations in harsh environment. Measurement 204:112179.

Jiang Y, Ding W, Gao Y, Gao Y (2022b) A new partial ambiguity resolution method based on modified solution separation and GNSS epoch-differencing. J Geod 96(11):88.

Kurum M, Farhad MM, Boyd D (2022) GNSS transmissometry (GNSS-T): modeling propagation of gnss signals through forest canopy. In: IGARSS 2022 - 2022 IEEE International Geoscience and Remote Sensing Symposium. pp 4695–4698

Opricovic S, Tzeng G-H (2004) Compromise solution by MCDM methods: A comparative analysis of VIKOR and TOPSIS. European Journal of Operational Research 156(2):445–455.

Wen Y, Dai W, Yu W, Chen B, Pan L (2024) An enhanced RANSAC-RTK algorithm in GNSS-challenged environments. Journal of Spatial Science :1–20.

Xi R, Xu D, Jiang W, He Q, Zhou X, Chen Q, Fan X (2023) Elimination of GNSS carrier phase diffraction error using an obstruction adaptive elevation masks determination method in a harsh observing environment. GPS Solut 27(3):139.

Yu J, Meng X, Yan B, Xu B, Fan Q, Xie Y (2020) Global Navigation Satellite System-based positioning technology for structural health monitoring: a review. Structural Control and Health Monitoring 27(1):e2467.

Zhang Z, Dong Y, Wen Y, Luo Y (2023a) Modeling, refinement and evaluation of multipath mitigation based on the hemispherical map in BDS2/BDS3 relative precise positioning. Measurement 213:112722.

Zhang Z, Li Y, He X, Chen W, Li B (2022) A composite stochastic model considering the terrain topography for real-time GNSS monitoring in canyon environments. J Geod 96(10):79.

Zhang Z, Zeng J, Li B, He X (2023b) Principles, methods and applications of cycle slip detection and repair under complex observation conditions. J Geod 97(5):50.